

2015

Synthesis and magnetism of single-phase Mn-Ga films

Wenyong Zhang

University of Nebraska-Lincoln, wenyong.zhang@unl.edu

Parashu Kharel

University of Nebraska-Lincoln, South Dakota State University, pkharel2@unl.edu

Shah R. Valloppilly

University of Nebraska-Lincoln, svalloppilly2@unl.edu

Ralph A. Skomski

University of Nebraska-Lincoln, rskomski2@unl.edu

David J. Sellmyer

University of Nebraska at Lincoln, dsellmyer@unl.edu

Follow this and additional works at: <http://digitalcommons.unl.edu/physicsellmyer>

 Part of the [Physics Commons](#)

Zhang, Wenyong; Kharel, Parashu; Valloppilly, Shah R.; Skomski, Ralph A.; and Sellmyer, David J., "Synthesis and magnetism of single-phase Mn-Ga films" (2015). *David Sellmyer Publications*. 252.

<http://digitalcommons.unl.edu/physicsellmyer/252>

This Article is brought to you for free and open access by the Research Papers in Physics and Astronomy at DigitalCommons@University of Nebraska - Lincoln. It has been accepted for inclusion in David Sellmyer Publications by an authorized administrator of DigitalCommons@University of Nebraska - Lincoln.

Synthesis and magnetism of single-phase Mn-Ga films

W. Y. Zhang,^{1,2,a)} P. Kharel,^{1,3} S. Valloppilly,¹ R. Skomski,^{1,2} and D. J. Sellmyer^{1,2}

¹Nebraska Center for Materials and Nanoscience, University of Nebraska, Lincoln, Nebraska 68588, USA

²Department of Physics and Astronomy, University of Nebraska, Lincoln, Nebraska 68588, USA

³Department of Physics, South Dakota State University, Brookings, South Dakota 57007, USA

(Presented 7 November 2014; received 22 September 2014; accepted 23 October 2014; published online 20 February 2015)

Single-phase noncubic Mn-Ga films with a thickness of about 200 nm were fabricated by an *in situ* annealing of [Mn(x)/Ga(y)/Mn(x)]₅ multilayers deposited by e-beam evaporation. Mn-Ga alloys prepared in three different compositions Mn₂Ga₅ and Mn₂Ga were found to crystallize in the tetragonal tP14 and tP2 structures, respectively. Mn₃Ga crystallizes in the hexagonal hp8 or tetragonal tI8 structures. All three alloys show substantial magnetocrystalline anisotropy between 7 and 10 Mergs/cm³. The samples show hard magnetic properties including coercivities of Mn₂Ga₅ and Mn₂Ga about 12.0 kOe and of Mn₃Ga about 13.4 kOe. The saturation magnetization and Curie temperature of Mn₂Ga₅, Mn₂Ga, and Mn₃Ga are 183 emu/cm³ and 435 K, 342 emu/cm³ and 697 K, and 151 emu/cm³ and 798 K, respectively. The samples show metallic electron transport up to room temperature. © 2015 AIP Publishing LLC. [<http://dx.doi.org/10.1063/1.4908022>]

INTRODUCTION

Mn-Ga compounds have recently attracted much attention because some of these alloys with non-cubic crystal structures exhibit substantial magnetocrystalline anisotropies and high Curie temperature, with potential for permanent magnet, high-density recording, and spin-based electronic devices.¹⁻⁴ Mn_{3-x}Ga (0 ≤ x ≤ 2) in the tetragonal and hexagonal structures and Mn₂Ga₅ in the tetragonal structure are the most common Mn-Ga-based phases. An interesting feature of these compounds is that their magnetic properties can be modified by adjusting the elemental compositions to fit a specific practical application. For example, Mn₃Ga in the tetragonal structure shows relatively small Mn moment (1.19 μ_B) and magnetic anisotropy (8.9 Merg/cm³) as compared to that of Mn₂Ga (2.08 μ_B/Mn and 23.5 Merg/cm³) in the tetragonal structure.⁵ However, Mn₃Ga in the hexagonal structure exhibits a triangular antiferromagnetic spin order at room temperature.⁶ On the other hand, tetragonal Mn₂Ga₅ has been reported to show ferromagnetism with high coercivity (H_c = 4 kOe at room temperature) and a magnetocrystalline anisotropy field of greater than 5 kOe.^{7,8} The observed high coercivity has been attributed to the presence of an unidentified secondary phase which pins the domain walls of the main Mn₂Ga₅ phase. Recently, a large net magnetization of about 1.36 μ_B/Mn has been reported for a Mn₂Ga₅ button annealed at 773 K.⁹

Our interest is to investigate structural, magnetic, and electron-transport properties of single-phase Mn₂Ga₅, Mn₂Ga, and Mn₃Ga films and compare their properties with those of the related compounds prepared by different methods.^{1,5} In this paper, we present our experimental investigation on the crystal structure, magnetic, and electron-transport properties of e-beam evaporated Mn₂Ga, Mn₃Ga, and Mn₂Ga₅ films.

EXPERIMENTAL METHODS

Mn₂Ga, Mn₃Ga, and Mn₂Ga₅ films with a thickness of about 200 nm were prepared by multilayer deposition and subsequent *in situ* annealing using an AJA e-beam evaporation system. Three samples with multilayer structures [Mn(6 nm)/Ga(28 nm)/Mn(6 nm)]₅, [Mn(13.7 nm)/Ga(12.7 nm)]/Mn(13.7 nm)]₅, and [Mn(15.3 nm)/Ga(9.4 nm)/Mn(15.3 nm)]₅ were deposited on glass substrates at 873 K to obtain the desired elemental compositions Mn₂Ga, Mn₃Ga, and Mn₂Ga₅, respectively. The Mn and Ga metals were evaporated at a constant rate of 4 Å/s. The Mn/Ga/Mn multilayer samples were annealed *in situ* at 1073 K for 1 h, and then were coated with a 20 nm-thick Ti layer to prevent oxidation. The total thicknesses of the annealed films were determined using a Bruker Dektak-XT stylus surface profiling system. Phase compositions were determined by X-ray diffraction (XRD). The magnetic and electrical transport properties of the films were investigated using the Quantum Design Magnetic Property Measurement System (MPMS) and Physical Property Measurement System (PPMS), respectively. The applied magnetic field is parallel to the film plane.

RESULTS AND DISCUSSION

Figure 1 shows the XRD patterns of the Mn-Ga films with various compositions and structures. As shown in Figs. 1(a) and 1(b), the diffraction peaks for the Mn₂Ga₅ and Mn₂Ga films can be indexed with the standard pattern for their tP14 and tP2 crystal structures.^{9,10} The XRD pattern of Mn₃Ga indicates that the film has crystallized into the hexagonal hp8 structure, Fig. 1(c). We note that Mn₃Ga can be stabilized in a hexagonal structure if it is cooled from a temperature exceeding 830 K, although the tetragonal phase is the most stable one and is obtained by a low-temperature heat treatment between 725 K and 825 K.¹¹ We have obtained the tetragonal Mn₃Ga by reannealing the *in situ* annealed sample at 800 K for 2 h. All films are

^{a)}Author to whom correspondence should be addressed. Electronic mail: wenyong.zhang@unl.edu.

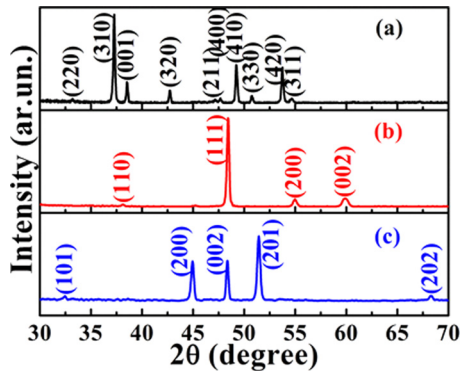


FIG. 1. XRD patterns of (a) tetragonal Mn_2Ga_5 , (b) tetragonal Mn_2Ga , and (c) hexagonal Mn_3Ga films.

polycrystalline and no elemental or alloy secondary phases were detected. The values of c/a for Mn_2Ga_5 , Mn_2Ga , and Mn_3Ga are 0.31, 0.92, and 0.81, respectively.

Figure 2 shows the magnetization as a function of temperature $M(T)$ for Mn_2Ga_5 , Mn_2Ga , and Mn_3Ga films, all in the tetragonal structure, measured between 300 K and 900 K at 1 kOe external field. The $M(T)$ curves are similar to those of ferro- or ferrimagnetic materials. All three $M(T)$ curves have single magnetic transitions (ferrimagnetic to paramagnetic). The Curie temperature (T_c) for the Mn_2Ga_5 phase is 435 K, close to the reported value,⁹ whereas that for the Mn_2Ga ($T_c = 679$ K) and Mn_3Ga ($T_c = 798$ K) phases are much higher than that of Mn_2Ga_5 . These high values of T_c compare well with those reported for corresponding bulk ingot and melt-spun ribbon samples.¹²

Figure 3 shows the magnetic-field dependence of magnetization $M(H)$ for the tetragonal and hexagonal Mn-Ga films measured at the room temperature. All tetragonal films (Mn_2Ga_5 , Mn_2Ga and Mn_3Ga) have a coercivity of about 12 kOe. This value of coercivity for Mn_2Ga_5 is much larger than that reported for its bulk counterpart with an unknown impurity phase.^{7,8} This suggests a high value of magnetic anisotropy in the phase-pure Mn_2Ga_5 films. The hexagonal Mn_3Ga shows a smaller coercivity of 3.3 kOe. The $M(H)$ loops of the tetragonal films indicate that the saturation magnetizations are approximately 342, 151, and 183 emu/cm^3 for Mn_2Ga , Mn_3Ga , and Mn_2Ga_5 , respectively.

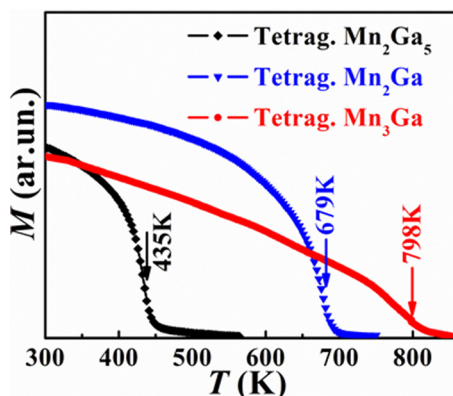


FIG. 2. $M(T)$ curves of tetragonal Mn_2Ga_5 , Mn_2Ga , and Mn_3Ga films.

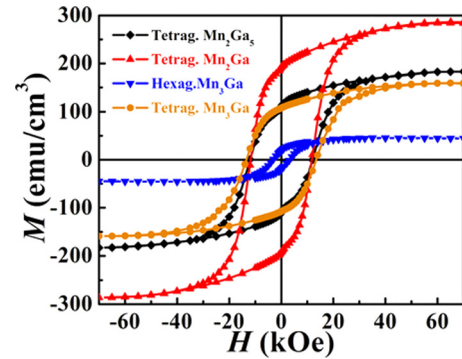


FIG. 3. Room-temperature hysteresis loops of the different Mn-Ga films.

We have determined the magnetocrystalline anisotropy constants K for the films in the tetragonal structure using the law-of-approach to saturation method, where the high-field part of the $M(H)$ loop is fitted with a standard equation to determine K and the saturation magnetization M_s .¹³ The values of K for tetragonal Mn_2Ga_5 , Mn_2Ga , and Mn_3Ga are 8, 10, and 7 Mergs/cm^3 and the corresponding values of M_s are 239, 359, and 175 emu/cm^3 , respectively. The magnetocrystalline anisotropy field $H_a = 67$ kOe for Mn_2Ga_5 film calculated using $2K/M_s$ is close to that of the hexagonal MnBi .¹⁴ The tetragonal Mn_2Ga film shows the highest value of magnetization in this series which may be attributed to the presence of a relatively high concentration of ferromagnetically coupled Mn-Mn pairs. The hexagonal Mn_3Ga film also shows small magnetic moment at room temperature, which may be attributed to the uncompensated triangular spins.¹⁵ However, the saturation magnetizations of these Mn-Ga films are smaller than those reported for their bulk counterparts.^{5,9} The low M_s in the films may be caused by the significant structural disorder.

Figures 4(a) and 4(b) show the temperature dependence of resistivity $\rho(T)$ of the tetragonal Mn_2Ga_5 and Mn_3Ga films measured at $H = 0$ kOe and $H = 70$ kOe. The resistivity was measured using the standard four-point probe method. Both the films are relatively poor metallic conductor with their room temperature resistivities being on the order of 1 $\text{m}\Omega/\text{cm}$; the resistivity of Mn_2Ga_5 film is slightly larger than that of the Mn_3Ga film. As the temperature decreases below 300 K, the resistivities of the films decrease almost linearly and pass through minima near 38 K. As shown in Fig. 4(b), the linear portion of the $\rho(T)$ curves of tetragonal Mn_3Ga (between 50 and 305 K) are fitted with an empirical relation $\rho = \rho_0 + aT^n$, where ρ_0 and a are constants. The value of the exponent n determined from the fit is 1.34. Below the minimum, the resistivity varies with temperature as a log function: $\rho = \rho_0 - c \ln(T^2 + \delta^2)$, where ρ_0 , c , and δ are constants as shown in Fig. 4(c).^{11,16} The values of the residual resistivity ratio (RRR) defined as $\rho_{305\text{K}}/\rho_{2\text{K}}$ for the Mn_2Ga_5 and Mn_3Ga films are close to one, indicating that the films have substantial structural disorder which would produce spin disorder because of likely antiferromagnetic Mn-Mn interactions. If the low-temperature spin structure has spin-glass-like feature, the conduction electrons may exhibit scattering from a nearly degenerate two-level system as

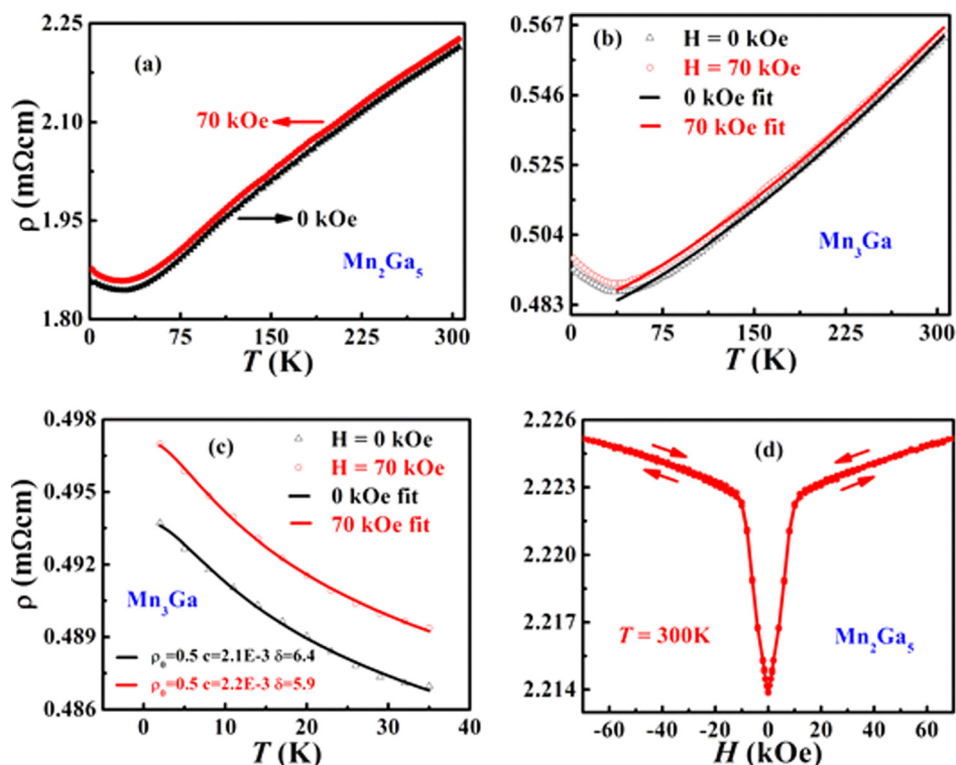


FIG. 4. Temperature dependent resistivity $\rho(T)$ of (a) tetragonal Mn_2Ga_5 film, and (b) tetragonal Mn_3Ga film measured at 0 and 70 kOe, where the solid lines in (b) fit an expression $\rho = \rho_0 + aT^n$ to the high-temperature (between 50 K and 300 K) resistivity data of tetragonal Mn_3Ga . (c) The low-temperature (between 2 K and 35 K) resistivity data of Mn_3Ga film fitted to a log function $\rho = \rho_0 - c \ln(T^2 + \delta^2)$. (d) Room-temperature $\rho(H)$ curves of the tetragonal Mn_2Ga_5 film.

suggested in Ref. 16. This type of low-temperature resistivity behavior has been observed in other Mn-based magnetic alloys such as disordered cubic Mn_3Ga .¹¹ Both samples show positive and small magnetoresistance (0.7% at room temperature). This may be attributed to the spin disorder due to competing ferro- and antiferromagnetic interactions present in the films. As shown in Fig. 4(d), the room-temperature resistivity of the Mn_2Ga_5 film increases rapidly with increasing magnetic field up to a critical field which is likely to be associated with the near saturation of magnetization, and then increases slowly with further increase in the external magnetic field.

CONCLUSIONS

Single-phase Mn-Ga films with composition Mn_2Ga_5 , Mn_2Ga , and Mn_3Ga in the tetragonal and hexagonal crystal structures have been synthesized using e-beam evaporation and subsequent *in-situ* annealing. All the tetragonal films show hard magnetic properties with coercivities of about 12 kOe and magnetocrystalline anisotropy constants of about 10 Mergs/cm³. Mn_2Ga shows the highest value (342 emu/cm³) of saturation magnetization. Hexagonal Mn_3Ga shows a small average magnetic moment at 300 K, probably due to uncompensated spins in its triangular spin structure. The magnetizations of the tetragonal Mn-Ga films are smaller than the values reported for bulk materials. All samples show metallic electron transport up to 305 K, and low-temperature resistance minima, which may be attributed to the presence of structural disorder and scattering from a two-level magnetic system. The origin of the small positive magnetoresistance in tetragonal Mn-Ga films is explained as originating from antiferromagnetically coupled Mn-Mn

pairs. Our results show that the tetragonal Mn-Ga films including Mn_2Ga_5 have potential for the applications of spin-transfer-torque memory and magnetic micro-electro-mechanical systems.

ACKNOWLEDGMENTS

W.Y.Z., R.S., and D.J.S. were financially supported by a Grant from the U.S. DOE-BES-DMSE (Grant No. DE-FG02-04ER46152, Program Directors M. Pechan, J. Horwitz). P.K. was supported by the NSF MRSEC (Grant No. DMR-0820521). Research was performed, in part, in Facilities of the Nebraska Center for Materials and Nanoscience, which is supported by the Nebraska Research Initiative.

- ¹H. Kurt, K. Rode, M. Venkatesan, P. Stamenov, and J. M. D. Coey, *Phys. Status Solidi B* **248**, 2338 (2011).
- ²S. Mizukami, F. Wu, A. Sakuma, J. Walowski, D. Watanabe, T. Kubota, X. Zhang, H. Naganuma, M. Oogane, Y. Ando, and T. Miyazaki, *Phys. Rev. Lett.* **106**, 117201 (2011).
- ³J. Winterlik, B. Balke, G. H. Fecher, C. Felser, M. C. M. Alves, F. Bernardi, and J. Morais, *Phys. Rev. B* **77**, 054406 (2008).
- ⁴L. J. Zhu, S. H. Nie, K. K. Meng, D. Pan, J. H. Zhao, and H. Z. Zheng, *Adv. Mater.* **24**, 4547 (2012).
- ⁵J. M. D. Coey, *J. Phys.: Condens. Matter* **26**, 064211 (2014).
- ⁶H. Kurt, K. Rode, H. Tokuc, P. Stamenov, M. Venkatesan, and J. M. D. Coey, *Appl. Phys. Lett.* **101**, 232402 (2012).
- ⁷T. Matsui, M. Suzuki, K. Morii, and Y. Nakayama, *J. Appl. Phys.* **73**, 6683 (1993).
- ⁸J. Aoki, K. Morii, T. Matsui, and Y. Nakayama, *Mater. Sci. Eng. B* **10**, L5 (1991).
- ⁹S. H. Kim, M. Boström, and D. K. Seo, *J. Am. Chem. Soc.* **130**, 1384 (2008).
- ¹⁰K. Schubert, H. G. Meissner, A. Raman, and W. Rossteutscher, *Naturwissenschaften* **51**, 287 (1964).
- ¹¹P. Kharel, Y. Huh, N. Al-Aqtash, V. R. Shah, R. F. Sabirianov, R. Skomski, and D. J. Sellmyer, *J. Phys.: Condens. Matter* **26**, 126001 (2014).

¹²Y. Huh, P. Kharel, V. R. Shah, E. Krage, R. Skomski, J. E. Shield, and D. J. Sellmyer, *IEEE Trans. Magn.* **49**, 3277 (2013).

¹³G. Hadjipanayis and D. J. Sellmyer, *Phys. Rev. B* **23**, 3349 (1981).

¹⁴X. Guo, X. Chen, Z. Altounian, and J. O. Ström-Olsen, *Phys. Rev. B* **46**, 14578 (1992).

¹⁵H. Niida, T. Hori, and Y. Nakagawa, *J. Phys. Soc. Jpn.* **52**, 1512 (1983).

¹⁶Y. Öner, O. Kamer, and J. H. J. Ross, *J. Appl. Phys.* **100**, 113910 (2006).